ISSN 0021-3640, JETP Letters, 2017, Vol. 106, No. 6, pp. 366–370. © Pleiades Publishing, Inc., 2017.
Original Russian Text © A.V. Mokshin, R.M. Khusnutdinov, A.R. Akhmerova, A.R. Musabirova, 2017, published in Pis'ma v Zhurnal Eksperimental'noi i Teoreticheskoi Fiziki, 2017, Vol. 106, No. 6, pp. 343–348.

CONDENSED MATTER

Universality of Microscopic Structural and Dynamic Features in Liquid Alkali Metals near the Melting Point

A. V. Mokshin*, R. M. Khusnutdinov, A. R. Akhmerova, and A. R. Musabirova

Kazan Federal University, Kazan, 420008 Russia

**e-mail: anatolii.mokshin@mail.ru*

Received August 18, 2017

The assumption proposed in [U. Balucani et al., Phys. Rev. B **47**, 3011 (1993)] that the space and time dependences of the characteristics of the microscopic structure and dynamics for the group of liquid alkali metals are reduced to a common general form through scaling transformations has been discussed. It has been found that such description is possible when scale units are (i) the effective size of a particle corresponding, in particular, to the experimentally measured position of the main peak in the static structure factor, (ii) the characteristic time scale of the thermal mean free path of the particle, and (iii) the parameters of the "liquid"–"crystal" phase separation (in particular, the melting temperature). This conclusion follows directly from the comparative analysis of experimental data on X-ray diffraction, as well as on the inelastic neutron and X-ray scattering data. This work develops the ideas proposed in [A. V. Mokshin et al., J. Chem. Phys. **121**, 7341 (2004)].

DOI: 10.1134/S0021364017180096

The statement that microscopically structurally dynamic features of liquids of a certain type (groups of liquefied inert gases Ar, Ne, Kr, Xe; groups of liquid single-component semiconductors with the same coordinate number, e.g., Ge, Si; liquid alkaline earth metals Be, Ca, Mg, Sr; liquid alkali metals; etc.) are universal for this type appears to be not so unambiguous as one could expect. This is most clearly seen in the case of ambiguous treatment of experimental data and results of molecular dynamics simulation for liquid alkali metals, which are typical representatives of the class of simple liquids [1–3].

According to the general concepts of the molecular kinetic theory, it is reasonable to expect that the general character of the interaction between particles in systems of a certain type in identical (equilibrium) thermodynamic phase states should generate a similar structure as well as the single-particle and collective dynamics of a similar character. These concepts underlie the development of theories (usually microscopic) for the description of microscopic dynamics, where one of the key input parameters is the potential of interaction between particles (as was done, e.g., for liquid alkali metals in [4]). It is remarkable that the molecular dynamics simulations [1] for liquid alkali metals (Na, K, Rb, and Cs) near the melting point with the Price–Singwi–Tosi model pseudopotential also indicate that static and dynamic structural correlations for all alkali metals are universally scaled. Earlier attempts at testing the manifestation of such "universality"[1] with theoretical and molecular dynamics considerations were reported in [5–9]. Nevertheless, the most reliable evidence of correctness of these considerations and conclusions could be their confirmation by experimental data. This became possible owing to the development of technique of inelastic X-ray scattering [10]. This technique allows obtaining the corresponding experimental data for liquid lithium [11], sodium [3, 12, 13], and potassium [14, 15] and, thereby, supplementing previous experimental results obtained with the inelastic neutron scattering for liquid potassium [16], rubidium [17], and cesium [18]. It is noteworthy that all these measurements provided the dynamic structure factor $S(k,\omega)$, which contains information on the structure and collective dynamics of particles with the characteristic time $t = 2\pi/\omega$ and spatial $\ell = 2\pi/k$ scales (here, ω and k are the frequency and wavenumber, respectively). Furthermore, an important feature of these experiments is that they were performed for melts at temperatures near the melting point (see Table 1). For this reason, the thermodynamic phase state of systems can be characterized by only the reduced temperature T/T_m, where T_m is the melting temperature of the corresponding system (see Table 1).

Comparing experimental spectra of the dynamic structure factor [2, 3, 19] and features of these spectra

[1] Corresponding to the so-called "principle of corresponding states" [1].

Table 1. Some physical parameters near the melting temperature T_m: density ρ_m, mass m, and effective size σ of the atom, reduced temperature of the considered states T/T_m, and spatial r_m and time t_m scale units

Parameter	Li	Na	K	Rb	Cs
T_m (K)	453.70	371.00	336.35	312.64	301.55
ρ_m (g/cm^3)	0.534	0.971	0.856	1.532	1.873
m (10^{-24} g)	11.5	38.2	64.9	141.9	221.0
σ (Å)	2.65	3.34	4.15	4.41	4.8.0
T/T_m	1.021	1.019	1.019	1.002	1.005
r_m (Å)	2.51	3.14	3.93	4.19	4.36
t_m (ps)	0.05	0.13	0.23	0.37	0.51

[20] for liquid alkali metals, different researchers arrived at different conclusions. In this work, in order to resolve existing contradictions, we analyze in detail existing experimental data on both the microscopic structure and dynamics of liquid alkali metals. It is obviously important to choose the corresponding parameters for scaling. It is reasonable to take the spatial scale unit in the form $r_m = 2\pi/k_m$, which corresponds to the effective size of particles in the system; here, k_m is the position of the main maximum of the static structure factor. Further, it is reasonable to take the time scale unit in the form $t_m = k^{-1}\sqrt{m/k_BT}$, where m is the mass of the particle. In other words, t_m is the time of the thermal mean free path of the particle at the spatial scale $\ell = 2\pi/k$. Correspondingly, the frequency scale unit is $\omega_m = 2\pi/t_m$.

Microscopic structure. The static structure factor $S(k)$ is the zeroth frequency moment (normalization condition) of the dynamic structure factor [21]:

$$S(k) = \int S(k,\omega)d\omega.$$

In the case of simple liquids, results for the static structure factor related to the radial distribution function of particles $g(r)$ through the sine or cosine Fourier transform,

$$S(k) = 1 + \frac{4\pi\rho}{k}\int_0^\infty r[g(r)-1]\sin(kr)dr$$

$$= 1 - \frac{4\pi\rho}{k}\frac{d}{dk}\int_0^\infty [g(r)-1]\cos(kr)dr,$$

can be directly compared because the static structure factor $S(k)$ is measured in neutron and X-ray diffraction experiments (ρ is the density). In particular, Fig. 1a shows experimental data for the static structure factor of liquid lithium, sodium, potassium, rubidium, and cesium near the melting point [22]; in this case, the static structure factor is represented as a function of the reduced wavenumber k/k_m. According to Fig. 1, experimental data for all considered systems can be described by a single dependence on k/k_m, which is quite expected. The intensities of peaks of the static structure factor $S(k)$, as well as their positions, in relative units are the same for all systems.

The radial distribution functions of atoms reconstructed from experimental data for $S(k)$ and recalculated with the reduced argument r/r_m are shown in Fig. 1b. These radial distribution functions for all systems are also reproduced by a single curve. It is remarkable that the function $g(r)$ does not manifest any crystal structure, including a structure with a bcc lattice typical of crystalline alkali metals [23]. The shape of the principal maximum of the function $g(r)$ does not include any features in the form of broadenings and "sholders." This property is typical of simple liquids where the interparticle (interatomic, ion–ion) interaction is correctly described by a spherical potential [24]. It is noteworthy that calculations with spherical pseudopotentials for liquid alkali metals are in better agreement with experimental data on the structure and dynamics than those with EAM many-body potentials [25–27]. The ratio of the so-called right to left half-width of the main maximum at the height $g(r) = 1$ gives the coefficient of asymmetry of the peak with the value $\sim 1.6 \pm 0.2$. The heights of the corresponding maxima $g(r)$ are the same for all systems, and for the first three maxima, we have

$$g(r_1) = 2.47 \pm 0.12, \quad g(r_2) = 1.26 \pm 0.03,$$
$$g(r_3) = 1.1 \pm 0.01.$$

The positions of the first three maxima $g(r)$ characterizing the first three pseudocoordination spheres (see Fig. 1b) are determined by the values

$$r_1/r_m = 1.17 \pm 0.01, \quad r_2/r_m = 2.2 \pm 0.03,$$
$$r_3/r_m = 3.19 \pm 0.04.$$

With an increase in the index of the pseudocoordination sphere, the width of the corresponding layer decreases. This is typical of a disordered system, where directional bonds in the interaction between particles are absent [28]. In particular, the widths of the first, second, and third coordination spheres, which are defined as the distances between the corresponding minima in the radial distribution function, are $\Delta r_1 \approx 1.6 r_m$, $\Delta r_2 \approx 1.06 r_m$, and $\Delta r_3 \approx 0.96 r_m$, respectively (see Fig. 1b).

Microscopic collective dynamics. The dynamic structure factor $S(k,\omega)$ for the inelastic neutron scattering can be extracted directly from the experimental data [21, 29]. At the same time, the intensity of inelas-

tic of X-ray scattering $I(k,\omega)$ defined as is the convolution of $S(k,\omega)$ with the experimental resolution function $R(k,\omega)$ [30]:

$$I(k,\omega) \propto \int R(k,\omega-\omega')\frac{\hbar\omega'/k_BT}{1-e^{-\hbar\omega'/k_BT}}S(k,\omega')d\omega'. \quad (1)$$

The intensity, as well as the dynamic structure factor, is measured in units of time (e.g., in seconds). Since the deconvolution of the integral expression in Eq. (1) and the extraction of $S(k,\omega)$ values are quite laborious, experimental data in this case are usually treated in terms of the scattering intensity $I(k,\omega)$ whose form (dependences on k and ω) completely corresponds to the form of $S(k,\omega)$. Such approach was implemented in [3] when comparing experimental data on inelastic X-ray scattering in liquid lithium and sodium (and aluminum).

For liquid alkali metals (lithium, sodium, and potassium) near the melting temperature, the experimental spectra of the intensity of scattering of X rays $I(k,\omega)$ [3, 11, 31] corresponding to different regions of the wavenumber k, but with maximally close k/k_m values, were selected and reduced to the dimensionless form $\omega_m I(k,\omega)$. Figure 2 shows these spectra for liquid lithium at a temperature of $T = 475$ K ($T/T_m = 1.049$), sodium melt at a temperature of $T = 390$ K ($T/T_m = 1.051$), and liquid potassium at a temperature of $T = 343$ K ($T/T_m = 1.020$).

According to Fig. 2, the spectra coincide with each other within the experimental errors. The shapes of the central and inelastic components of the intensities $\omega_m I(k,\omega)$ for melts are almost identical. All these features indicate that the microscopic dynamics of liquid alkali metals in the corresponding states is universal and the collective atomic dynamics of liquid alkali metals can be theoretically described with general scaling laws.

As is known, the position of the high-frequency peak $\omega_c(k)$ in spectra of the dynamic structure factor $\omega_c(k)$ correlates with the position of the high-frequency peak in the spectral density of the longitudinal flux $C_L(k,\omega)$ and, thereby, corresponds to the dispersion law of acoustic vibrations with longitudinal polarization [32, 33]. Following [20] and assuming that the positions of high-frequency peaks in the spectra of the intensity $I(k,\omega)$ and the spectra of the dynamic structure factor $S(k,\omega)$ are close to each other, one can estimate dispersion laws for liquid alkali metals using data on inelastic X-ray scattering (for lithium [11], sodium [3], and potassium [31]) and on inelastic neutron scattering (for rubidium [17] and cesium [18]).

The dispersion curves $\omega_c(k)$ for liquid alkali metals are shown in Fig. 3a. This figure clearly demonstrates similarity in the dispersion laws and the following property: as the atomic number increases, the position

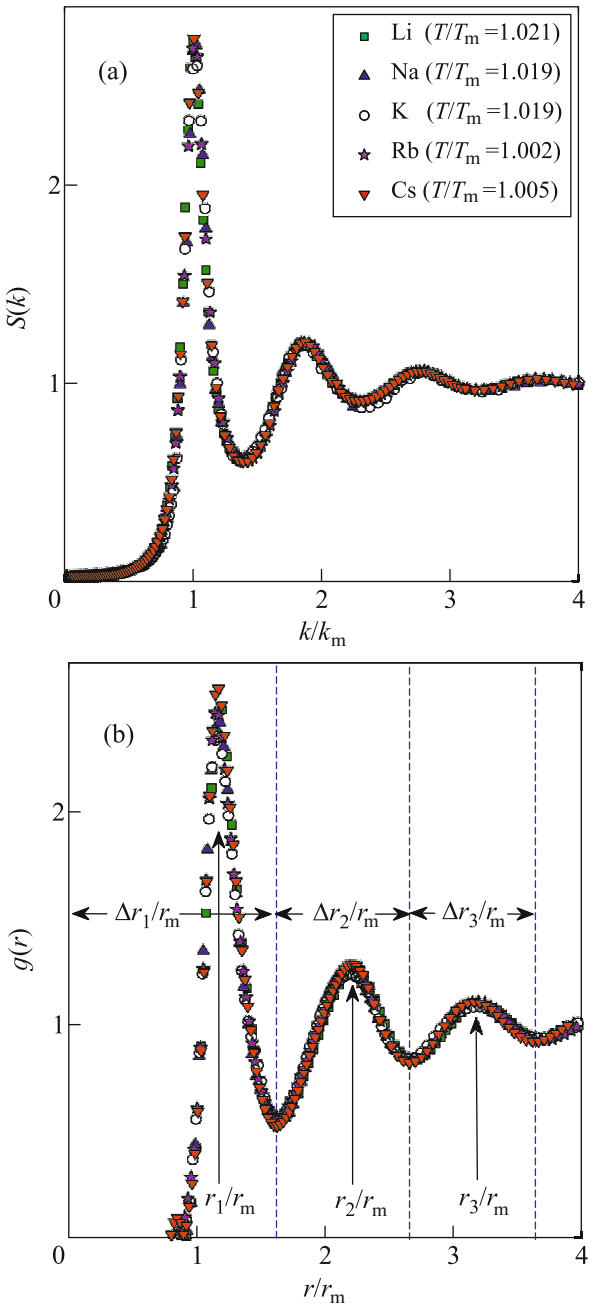

Fig. 1. (Color online) (a) Static structure factor $S(k)$ versus the reduced wavenumber k/k_m and (b) radial distribution of particles $g(r)$ versus the reduced distance r/r_m in liquid alkali metals [22].

of the maximum k_{max} is shifted toward lower k values and the height of the maximum ω_{max} of the dispersion curves decreases. Furthermore, as is seen in the insets, the quantities k_{max} and ω_{max} directly correlate with the scale units k_m and ω_m estimated for liquid alkali metals. This correlation indicates a universal character of the dispersion law inside this group of liquids (see also

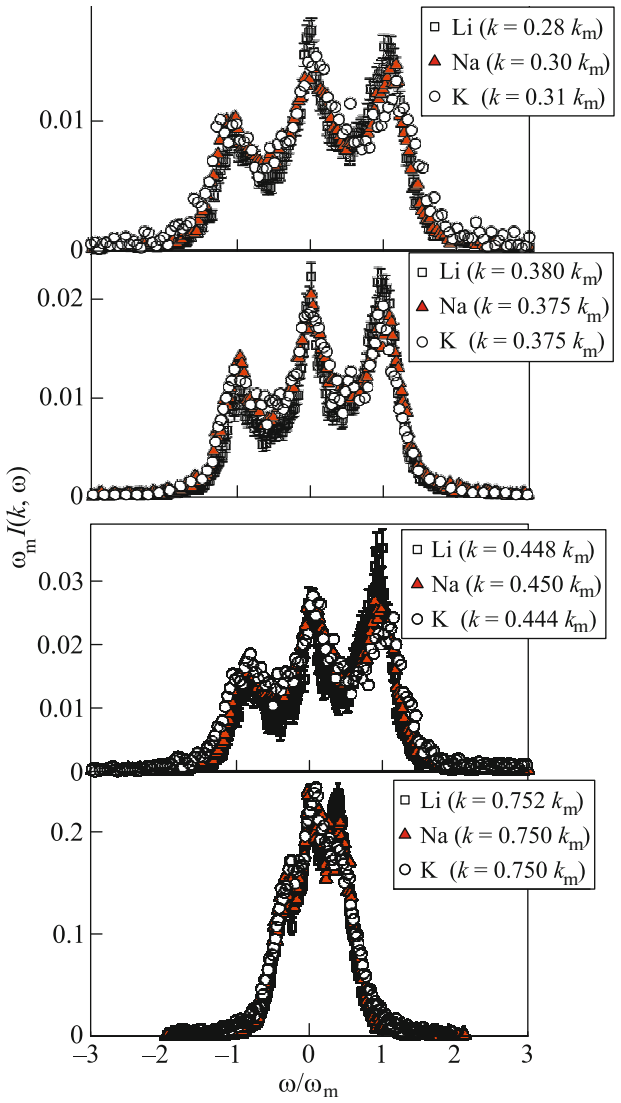

Fig. 2. (Color online) Spectra of inelastic scattering of X rays for liquid lithium at a temperature of $T = 475$ K, sodium melt at a temperature of $T = 390$ K, and liquid potassium at a temperature of $T = 343$ K [3, 11, 31] at different wavenumbers k. The experimental errors of the intensity are shown only for liquid lithium.

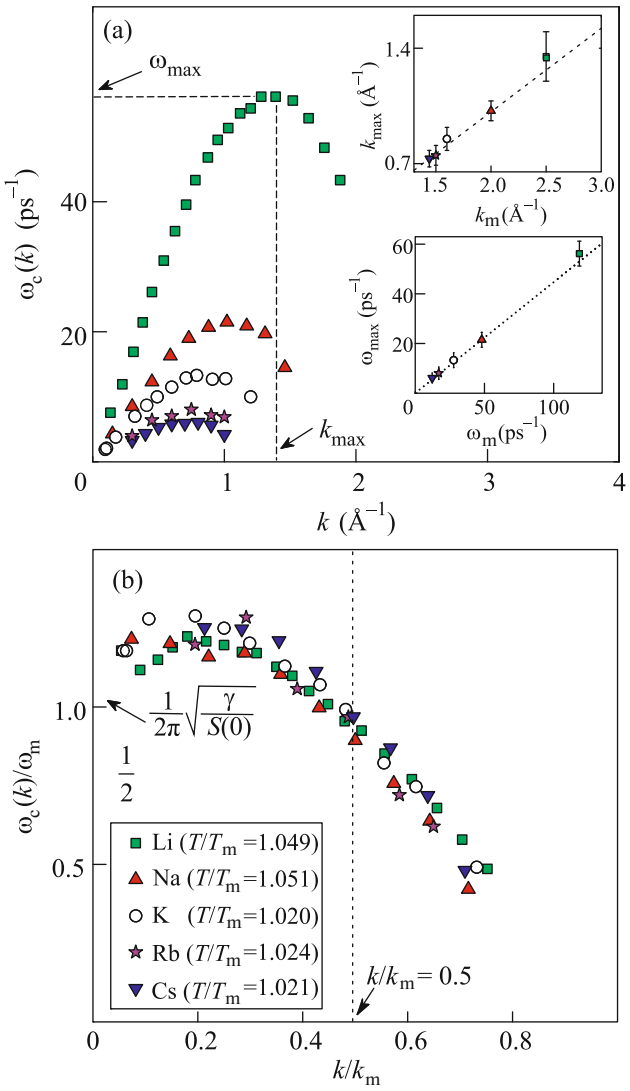

Fig. 3. (Color online) (a) Dispersion relation of the high-frequency peak $\omega_c(k)$ in the scattering spectra of liquid alkali metals. The upper inset shows the correlation between the position of the maximum k_{max} in the dispersion relation and the scale unit k_m. The lower inset shows correlation between the maximum in the dispersion relation ω_{max} and the frequency scale unit ω_m. (b) Dispersion relation of the high-frequency peak in reduced units. The vertical dashed straight line at $k/k_m = 0.5$ corresponds to the boundary of the first Brillouin zone.

Fig. 5 in [20]). The dispersion curves recalculated in reduced units k_m and ω_m are shown in Fig. 3b. Although these curves in this representation have a blurred maximum at very low wavenumbers $k/k_m \simeq 0.2 \pm 0.05$, which is unusual for dispersion laws, the common character of dispersion laws for these melts is obvious. Moreover, this maximum in the dispersion curve $\omega(k/k_m)/\omega_m$ correlates with the effect of so-called positive sound dispersion well known in the microscopic dynamics of liquids [34]. Small differences in the low-k region are significantly due to errors of experimental data, which complicate the estimation of exact ω_c values. This result has an important consequence. For example, for the low-k limit, we obtain

$$\lim_{k\to 0}\frac{\omega_c(k)}{\omega_m} = \frac{c_s}{2\pi}\sqrt{\frac{m}{k_B T}}, \qquad (2)$$

where c_s is the adiabatic speed of sound.

Then, taking into account that $v_T = \sqrt{3k_BT/m}$ and $c_s(0) = \sqrt{\gamma k_BT/[mS(0)]}$, where $\gamma = c_p/c_v$ is the ratio of specific heats, we find

$$\lim_{k\to 0}\frac{\omega_c(k)}{\omega_m} = \frac{\sqrt{3}}{2\pi}\frac{c_s}{v_T} = \frac{1}{2\pi}\sqrt{\frac{\gamma}{S(0)}}. \quad (3)$$

Here, the first equality means that the ratio of the adiabatic speed of sound c_s to the thermal velocity of particles v_T for liquid alkali metals in *the corresponding thermodynamic states* is the same. In particular, using the known c_s values for liquid lithium, sodium, potassium, rubidium, and cesium (see, e.g., Table 1 in [30]), we obtain $\omega_c(0)/\omega_m \simeq 1.1 \pm 0.13$. The second equality in Eq. (3) makes it possible, in particular, to determine the static structure factor in the low-k limit, $S(0) = \lim_{k\to 0} S(k)$, with known γ values, which for liquid metals are presented, e.g., in [30]. For example, $S(0) = 0.0295$ for liquid lithium, $S(0) = 0.0246$ for liquid sodium, $S(0) = 0.0229$ for liquid potassium, and $S(0) = 0.0227$ for liquid cesium.

We are grateful to Acad. V.V. Brazhkin, V.N. Ryzhov (Institute for High Pressure Physics, Russian Academy of Sciences, Troitsk, Moscow, Russia), and A.G. Novikov (Obninsk, Russia) for stimulating discussions and recommendations and to T. Scopigno (Università di Roma "La Sapienza," Roma) for presented experimental inelastic X-ray scattering data. This work was supported by the Ministry of Education and Science of the Russian Federation (subsidy to Kazan Federal University for the state scientific assignment no. 3.2166.2017/4.6). The work of A.V.M. was supported by the Council of the President of the Russian Federation for State Support of Young Scientists and Leading Scientific Schools (project no. MD-5792.2016.2).

REFERENCES

1. U. Balucani, A. Torcini, and R. Vallauri, Phys. Rev. B **47**, 3011 (1993).
2. T. Scopigno, U. Balucani, G. Ruocco, and F. Sette, J. Non-Cryst. Solids **312–314**, 121 (2002).
3. T. Scopigno, U. Balucani, G. Ruocco, and F. Sette, Phys. Rev. E **65**, 031205 (2002).
4. K. N. Lad and A. Pratap, Phys. Rev. E **73**, 054204 (2006).
5. R. D. Mountain, Inst. Phys. Conf. Ser. **30**, 62 (1977).
6. M. J. Huijben and W. van der Lugt, Acta Crystallogr. A **35**, 431 (1979).
7. H. B. Singh and A. Holtz, Phys. Rev. A **28**, 1108 (1983).
8. N. Matsuda, H. Mori, K. Hoshino, and M. Watabe, J. Phys.: Condens. Matter **3**, 827 (1991).
9. W. Schirmacher, B. Schmid, and H. Sinn, Eur. Phys. J. Spec. Top. **196**, 3 (2011).
10. E. Burkel, *Inelastic Scattering of X-rays with very High Energy Resolution* (Springer, Berlin, 1991).
11. T. Scopigno, U. Balucani, G. Ruocco, and F. Sette, J. Phys.: Condens. Matter **12**, 8009 (2000).
12. W.-C. Pilgrim, S. Hosokawa, H. Saggau, H. Sinn, and E. Burkel, J. Non-Cryst. Solids **250–252**, 96 (1999).
13. A. V. Mokshin, R. M. Yulmetyev, T. Scopigno, and P. Hänggi, J. Phys.: Condens. Matter **15**, 2235 (2003).
14. A. Monaco, T. Scopigno, P. Benassi, A. Giungi, G. Monaco, M. Mardone, G. Ruocco, and M. Sampli, J. Non-Cryst. Solids **353**, 3154 (2007).
15. L. E. Bove, B. Dorner, C. Petrillo, S. Sacchetti, and J.-B. Suck, Phys. Rev. B **68**, 024208 (2003).
16. A. G. Novikov, V. V. Savostin, A. L. Shimkevich, and M. V. Zaezjev, Physica A **234–236**, 359 (1997).
17. J. R. D. Copley and J. M. Rowe, Phys. Rev. Lett. **32**, 49 (1974).
18. T. Bodensteiner, C. Morkel, P. Müller, and W. Gläser, J. Non-Cryst. Solids **117–118**, 116 (1990).
19. A. V. Mokshin, R. M. Yulmetyev, and P. Hänggi, J. Chem. Phys. **121**, 7341 (2004).
20. N. M. Blagoveshchenskii, A. G. Novikov, and V. V. Savostin, Phys. Solid State **52**, 969 (2010).
21. P. A. Egelstaff, *An Introduction to the Liquid State* (Academic, New York, 1967).
22. Y. Waseda, *The Structure of Non-Crystalline Materials: Liquids and Amorphous Solids* (McGraw-Hill, New York, 1980).
23. T. Iida and R. I. L. Guthrie, *The Thermophysical Properties of Metallic Liquids,* Vol. 1: *Fundamentals* (Oxford Univ. Press, Oxford, 2015).
24. A. V. Mokshin, R. M. Khusnutdinov, A. G. Novikov, N. M. Blagoveshchenskii, and A. V. Puchkov, J. Exp. Theor. Phys. **121**, 828 (2015).
25. R. M. Khusnutdinov, A. V. Mokshin, and R. M. Yulmetyev, J. Exp. Theor. Phys. **108**, 417 (2009).
26. D. K. Belashchenko, *Computer Modeling of Liquid and Amorphous Substances* (MISIS, Moscow, 2005) [in Russian].
27. A. V. Mokshin, R. M. Khusnutdinov, and B. N. Galimzyanov, in preparation.
28. V. V. Brazhkin, Phys. Usp. **52**, 369 (2009).
29. R. M. Yulmetyev, A. V. Mokshin, P. Hänggi, and V. Yu. Shurygin, JETP Lett. **76**, 147 (2002).
30. T. Scopigno, G. Ruocco, and F. Sette, Rev. Mod. Phys. **77**, 881 (2005).
31. A. Monaco, T. Scopigno, P. Benassi, A. Giugni, G. Monaco, M. Nordone, G. Ruocco, and M. Sampoli, J. Chem. Phys. **120**, 8089 (2004).
32. N. H. March, *Liquid Metals: Concepts and Theory* (Cambridge Univ. Press, Cambridge, 1990).
33. A. V. Mokshin and R. M. Yul'met'ev, *Microscopic Dynamics of Simple Liquids* (Tsentr Innovats. Tekhnol., Kazan', 2006) [in Russian].
34. Yu. D. Fomin, V. N. Ryzhov, E. N. Tsiok, V. V. Brazhkin, and K. Trachenko, J. Phys.: Condens. Matter **28**, 43LT01 (2016).

Translated by R. Tyapaev